PHYSICAL REVIEW B **70**, 024103 (2004)

# Thermodynamics from *ab initio* computations

W. Zhang,[1,3] J. R. Smith,[2] and X.-G. Wang[2]
[1]*Materials Department, University of California, Santa Barbara, California 93106, USA*
[2]*Delphi Research Laboratories, Shelby Township, Michigan 48315, USA*
[3]*Institute of Ceramics, Chinese Academy of Sciences, Shanghai 200050, China*

(Received 10 December 2003; published 9 July 2004)

Links are established between the standard states and variables of thermodynamics and those of *ab initio* methods. This is a potentially powerful connection, not only improving the link between thermodynamics and atomic-level computations, but also increasing the predictability of *ab initio* techniques. The free energies connecting *ab initio* and thermodynamic standard states are called connection energies. Standard state connection energies for solids are written in terms of specific heats and entropies of the solids. Gaseous state connection energies can be written in terms of either gaseous properties or in terms of properties of the solids that are in thermodynamic equilibrium with the gases. Having two different references for these energies improves the robustness of the method. Equating these two gaseous connection energy expressions yields a simple relationship that must be obeyed by solid formation entropies. Finally, an *ab initio* structural phase diagram of ultrathin $\mathrm{Al}_x\mathrm{O}_y$ films on Al-doped Cu(111) is obtained.

DOI: 10.1103/PhysRevB.70.024103 PACS number(s): 65.40.−b, 68.35.−p

## I. INTRODUCTION

In recent years,[1–12] *ab initio* calculations combined with thermodynamic concepts have become an important strategy in structure stability analyses of complex materials that can involve intrinsic nonstoichiometries of the chemical compositions. *Ab initio* computations yield first-principles solutions of the Schrödinger equation without depending on empirical input. These computations cover a wide range of problems in surface structures,[1] defect stability,[2,3] doping[4] of semiconductors, oxide surfaces,[5–9] metal/oxide interfaces,[9–11] and even spintronics.[12] The *ab initio* strategy is to seek the state with the lowest Gibbs energy $G_s$ depending on the free energy of an ensemble $G_o$ as well as on chemical potentials $\mu_i$ of constituents,[13,14] i.e.,

$$G_S = G_o - N_1\mu_1 - N_2\mu_2 - N_3\mu_3 - \cdots . \tag{1}$$

Here $G_o$ is the free energy of the ensemble that may contain a nonstoichiometric structure such as a defect complex, surface, or interface. $\mu_i$ $(i=1,2,3,\ldots)$ are the chemical potentials of the constituents $i$ and $N_i$ are the corresponding atom numbers in the ensemble.

In this *ab initio* approach,[1–12] Eq. (1) is rewritten as

$$G_S = G_o - \Sigma_i N_i \mu_i^0(0\ K,p) - \Sigma_i N_i \Delta\mu_i \tag{2}$$

where the *ab initio* standard solid state chemical potential $\mu_i^0(0\ K,p)$ is the zero-temperature chemical potential of the *pure* material $i$ (containing single or multiple elements), at pressure $p$. For solids, the pressure dependence is normally weak enough to be ignored,[13,15] and $\mu_i^0(0\ \mathrm{K})$ can be obtained by *ab initio* computation. For a gas species, the *ab initio* standard state chemical potential $\mu_i^0(0\ \mathrm{K},p)$ is determined via quantum chemistry computations for an isolated molecule, but it remains to determine the thermodynamic counterpart to the isolated molecule. For clarity, the $\mu_i^0$(0 K, isolated) are employed to represent the chemical potentials of such theoretical standard states. Therefore the *ab initio* effective chemical potential differences $\Delta\mu_i$ are defined as

$$\text{Solids:}\Delta\mu_i = \mu_i - \mu_i^0(0\ \mathrm{K}), \tag{3a}$$

$$\text{Gases:}\Delta\mu_i = \mu_i - \mu_i^0(0\ \mathrm{K,isolated}). \tag{3b}$$

Here the *ab initio* standard states are defined such that $\mu_i^0(0\ \mathrm{K})$ are the total energies per atom of corresponding crystalline solids and the $\mu_i^0$(0 K, isolated) are the total energies per molecule of corresponding isolated gas molecules.[15] The $\Delta\mu_i$ can be used as effective variables to describe the environmental dependences of gases and solids.

Thermodynamic variables employed for metallurgical[13,14,16–22] and gas-solid interaction systems[13,23–26] are typically activities $a_i$ or partial pressures $p$, while *ab initio* approaches are more likely based on chemical potentials $\mu$ as discussed above. These variables can be related as[13]

$$\text{Solids:}\mu_i(\mathrm{T}) - \mu_i^0(\mathrm{T}) = k\mathrm{T}\ln a_i, \tag{4a}$$

$$\text{Gases:}\mu_i(\mathrm{T}) - \mu_i^0(\mathrm{T},p_i^0 = 1\ \mathrm{atm}) = k\mathrm{T}\ln p_i, \tag{4b}$$

where $k$ is Boltzmann's constant. Here the thermodynamic standard state for a solid is for a crystalline solid at temperature $T$ (not limited to $T=0$ K as is the *ab initio* standard state). In Eq. (4a), $\mu_i^0(T)$ corresponds to the chemical potential of a thermodynamic standard state solid. For a gas, the thermodynamic standard state is found at a pressure $P_i^0 = 1$ atm and temperature $T$. In Eq. (4b), $\mu_i^0(T,p_i^0=1\ \mathrm{atm})$ is the chemical potential of the thermodynamic standard state gas.[13] Here the chemical potential $\mu_i$ of the constituent $i$ depends on the temperature and its activity $a_i$ for solids (referring to the corresponding crystalline solid)[10,11,13,14] or its partial pressure $p_i$ for gases (referring to the corresponding molecular gas).[13] In metallurgical systems, the activity $a_i$ is related to the solute concentration of the constituent, $X_i$, (units are mole fraction), through the activity coefficient, $\gamma_i$

©2004 The American Physical Society

$\equiv a_i/X_i$.[13,16] For an ideal solid solution, the activity coefficient is unity and $a_i$ becomes the concentration in the solid solution.

Note the *ab initio* standard state for a gas (0 K, isolated) is rather artificial. In one's typical experience, as the temperature of a gas is lowered, it will first condense into a liquid state and subsequently into a solid state. Nevertheless, it will be shown in the following that there is a consistent procedure to connect between the *ab initio* standard state for gases and real gases at higher temperatures.

The connection between *ab initio* computations and thermodynamics also involves certain assumptions regarding thermodynamic equilibrium in actual applications. Thermodynamic equilibrium implies that the thermodynamic state variables are time independent and that the chemical potentials $\mu_i$ of each species are position independent. This may not be true for an entire system in practice, and one often finds in the literature (see, e.g., Refs. 1–12, 27) that a local equilibrium is assumed. For example, it is assumed that there is a local thermodynamic equilibrium between the interface region and a region of the bulk materials in the vicinity of the interface.[10] This assumed equilibrium region might be broadened to include the ambient gas so that the ambient gas partial pressures $p_i$, as well as the activities $a_i$ of material components are included as metallurgical variables in Eq. (4). For this to be a valid assumption, the temperature must be high enough so that kinetic rates are sufficiently fast that the atomic rearrangements necessary to maintain equilibrium can occur during the experiment.[27] For example, if the surface were flashed annealed and then low temperature measurements (below room temperature) were carried out as the sample cools, one would need to be concerned about the assumption of thermodynamic equilibrium. Also, equilibrium between an ambient gas species and a solid surface implies that the chemical potentials of the species in the gas and the corresponding species chemisorbed on the surface were the same. This implies that $\Delta H = T\Delta S$, where $\Delta H$ is the difference in enthalpy of the species between the gas phase and the surface phase and $\Delta S$ is the corresponding difference in entropy. Since $\Delta H$ can be substantial in this case, as $T$ decreases the entropy difference $\Delta S$ must be sufficiently large enough to maintain equilibrium. Alternatively, $T$ must be sufficiently high enough for the assumption of thermodynamic equilibrium to be valid in this case. While the assumption of thermodynamic equilibrium is often made in the field, one must bear the above in mind as we proceed.

In summary, one must be aware of the need for thermodynamic equilibrium, on a global or at least on a local scale, in the application of thermodynamics to solids and gases. Equations (3) and (4) indicate that the differences between the metallurgical and *ab initio* standard states are as follows. First, the *ab initio* solid standard state is limited to $T=0$ K, while the metallurgical standard state is defined for whatever temperature $T$ is of interest. Second, the *ab initio* treatment of a gaseous molecule is typically done for an isolated molecule, while the thermodynamic standard state pressure is defined at 1 atm. Third, the *ab initio* variables are the chemical potential differences $\Delta\mu_i$, referring to theoretical standard states, while the metallurgical variables are the activities $a_i$ and gas pressures $p_i$, referring to the thermodynamic standard state.

Bridging the gap between the *ab initio* variables and metallurgical variables requires the following two relations:

$$\text{Solids:}\mu_i^0(T) = \mu_i^0(0\text{ K}) + \Delta_i^o(T), \tag{5a}$$

$$\text{Gases:}\mu_i^0(T,p_i^0 = 1\text{ atm}) = \mu_i^0(0\text{ K,isolated}) + \Delta_i^o(T,p_i^0 = 1\text{ atm}). \tag{5b}$$

By combining Eqs. (3)–(5), the chemical potential $\mu_i$ of a constituent in a thermodynamical or metallurgical system can be linked directly to $\mu_i^0(0\text{ K})$ [or $\mu_i^0$ (0 K, isolated)], and to the measured activity $a_i$ (or the partial pressure $p_i$), through the quantities $\Delta_i^o$, which actually provide a key part of the bridge between thermodynamics and the results of *ab initio* calculations. We will call these $\Delta_i^o(T)$ and $\Delta_i^o(T,p_i^0)$ connection energies. Note that the above relationships are expressed in a general form, independent of any specific system.

An expression for the solid state connection energy $\Delta_i^o(T)$ has been obtained[10] for Eqs. (4a) and (5a). Some progress has also been made toward the gaseous state connection energy $\Delta_i^o(T,p_i^0=1\text{ atm})$. Consider a localized binary system, such as $Al_xO_y$ e.g., in the form of a thin film. When that binary system is at equilibrium with a bulk solid (thermodynamic reservoir) of the same constituents (e.g., $Al_2O_3$), linking the partial pressure of one constituent (e.g., oxygen), with a gaseous reference state and the other constituent to a solid reference state (e.g., Al), has been solved.[10]

More generally, for certain systems like semiconductor surfaces, oxide surfaces, metal/oxide interfaces, or other localized systems of interest, one may usually assume that the localized region is in equilibrium with a substrate or other solid reservoir that is a specific metal, ceramic, or semiconductor. However, for systems that do not have a simple solid reservoir of the same material, such as an ultrathin film on a heterogeneous substrate[28–30] or a structure at nanoscale, localized nonstoichiometric surface or interfacial phenomena may exist, but linking the chemical potential of the constituent with a gaseous reference state to the partial pressure of the reference state is not straightforward. Another complexity arises for systems that contain multiple constituents, some of which having only gaseous reference states, such as hydrogen in an oxide surface in the presence of an ambient containing oxygen and water vapor.[6,7,23,24,31,32]

In the following we will address the problem of connecting theoretical chemical potentials of those constituents with measured partial pressures, as is necessary for those constituents that have only gaseous reference states. We will also formulate the relationships appropriate for a constituent that has a solid state reference. This is essential for connecting *ab initio* thermodynamics with experimental observables.

## II. CONNECTING CHEMICAL POTENTIALS TO ACTIVITIES AND AMBIENT PARTIAL PRESSURES

### A. Constituent having a solid state reference

For a solid, the connection energy $\Delta_i^o(T)$ can be derived[10,13,14] from its specific heats $C_P$ as

$$\Delta_i^o(T) = [H_i^0(T) - H_i^0(0\ \mathrm{K})] - TS_i^0(T) = \int_0^T C_P dT - T\int_0^T (C_P^i/T)dT. \tag{6}$$

Here $H_i^0(T)$ is the enthalpy and $s_i^0(T)$ the entropy of a solid element $i$ at temperature $T$. Because most material data sets of these quantities are based on a room temperature reference state,[13,14] $T_r = 298.15$ K Eq. (6) is rewritten as

$$\Delta_i^o(T) = \Delta_i^o(T_r) + \left[\int_{T_r}^T C_P^i dT, - (T - T_r)S_i^0(T_r) - T\int_{T_r}^T (C_P^i/T)dT\right], \tag{7a}$$

with

$$\Delta_i^o(T_r) = [H_i^0(T_r) - H_i^0(0\ \mathrm{K})] - T_r S_i^0(T_r). \tag{7b}$$

Based on the connection energies $\Delta_i^o(T)$ now being determined, the theoretical $\Delta\mu_i$ can be related to a measured activity $a_i$ via Eqs. (3a), (4a), and (5a):

$$\Delta\mu_i = k\mathrm{T}\ \ln\ a_i + \Delta_i^0(\mathrm{T}). \tag{8}$$

### B. Constituent having a gaseous state reference

#### 1. Equilibrium with a binary bulk substrate

Many problems relate to the equilibrium of a system under investigation with a binary compound substrate. Consider the case where one constituent, $A$, in the system has a solid state reference, and the other constituent, $B$, has a gaseous reference state. The relationship between the activity of $A$, $a_A$, and the partial pressure $p_B$ can be determined by employing the reaction energy of the solid $A_xB_y$ as a bridge. For example, in the study of $Al_2O_3$ surfaces or metal/$Al_2O_3$ interfaces, linking to the partial pressure of $O_2$ can be bridged via the activity of Al.[10] More generally, when a system is in thermodynamic equilibrium with the solid (reservoir) $A_xB_y$, the activities $a_A$ and $a_B$ are coupled by

$$a_B = a_A^{-x/y}\exp\left[\left(\frac{1}{y}\right)\Delta G^0_{A_xB_y}/kT\right], \tag{9}$$

or

$$kT\ \ln\ a_A = \left(\frac{1}{x}\right)\Delta G^0_{A_xB_y} - \left(\frac{y}{x}\right)kT\ \ln\ a_B, \tag{10}$$

where $\Delta G^0_{A_xB_y}$ is the standard reaction energy of the solid $A_xB_y$, in accordance with the reaction,

$$xA(\mathrm{Solid}) + yB(\mathrm{gas}) = A_xB_y(\mathrm{solid}). \tag{11}$$

When thermodynamic equilibrium exists with a solid state reference and when, in addition, the system is in equilibrium with an environment containing the gas phase of $B$, the relationship to the partial pressure $p_B$ can be obtained from its activity in the solid $a_B$. Taking gaseous oxygen as an example ($B = O_2$), a relation $p_{O_2} = a_{O_2}$ exists in the ideal gas approximation.[33] Therefore, the reference to an isolated molecule (the standard *ab initio* reference state), is avoided by using the activity $a_A$ as a bridge, i.e.,

$$kT\ \ln\ a_A = \left(\frac{1}{x}\right)\Delta G^0_{A_xO_y} - \left(\frac{y}{x}\right)\ kT\ \ln\ P_{O_2}. \tag{12}$$

#### 2. A more general relationship

In Sec. II B 1, the link to the gas partial pressure [Eq. (12)] was established based on the assumption that there is thermodynamic equilibrium with a solid bulk reservoir. One might inquire how to elucidate the relationship between the measured gas partial pressure and the chemical potential in the absence of a solid bulk reservoir. This is a central issue of this paper, and we show how to determine a general $\Delta_i^o(T, p_i^0)$ for that purpose via solid state compound formation energies.

Let us begin from the definition of the Gibbs reaction energy of an arbitrarily chosen solid compound $A_xB_y$,[13] i.e.,

$$\Delta G^0_{A_xB_y}(T) = G^0_{A_xB_y}(T) - x\ \mu_A^0(T) - y\mu_B^0(T, p_B^0 = 1\ \mathrm{atm}), \tag{13}$$

which corresponds to the standard chemical reaction of Eq. (11). By Eqs. (5a) and (5b), we obtain

$$\Delta_B^0(T, p_B^0 = 1\ \mathrm{atm}) = \left(\frac{1}{y}\right)[\Delta H^{theo}_{A_xB_y}(0\ \mathrm{K}) - \Delta G^0_{A_xB_y}(T) + \Delta^0_{A_xB_y}(T) - x\Delta_A^0(T)], \tag{14}$$

with

$$\Delta H^{theo}_{A_xB_y}(0\ \mathrm{K}) = \mu^0_{A_xB_y}(0\ \mathrm{K}) - x\mu_A^0(0\ \mathrm{K}) - y\mu_B^0(0\ \mathrm{K, isolated}). \tag{15}$$

$\Delta H^{theo}_{A_xB_y}(0\ \mathrm{K})$ is *theoretical* heat of formation of the compound $A_xB_y$ that can be obtained by *ab initio* quantum chemistry calculations.[34] For the connection energy, a gas partial pressure of $p_B^0 = 1$ atm has been taken for convenience of comparison with standard state experimental data later. Note that Eq. (14) does not require that an equilibrium exists between the localized system of interest (e.g., a surface or interface) and a corresponding bulk substrate as a reservoir. The Gibbs reaction energy $\Delta G^0_{A_xB_y}(T)$ has been measured and tabulated in a handbook[14] for many compounds. Both $\Delta_A^0(T)$ and $\Delta^0_{A_xB_y}(T)$ can be determined by Eq. (6). Equation (14) combines experimental data on *solids* and a theoretical heat of formation to determine $\Delta_B^0(T, p_B^0 = 1\ \mathrm{atm})$. With the $\Delta_B^0(T, p_B^0 = 1\ \mathrm{atm})$ so determined, the problem of linking the theoretical chemical potential of a constituent to its partial pressure is solved in terms of solid compound formation energies. Taking water vapor as an example, Eq. (14) becomes

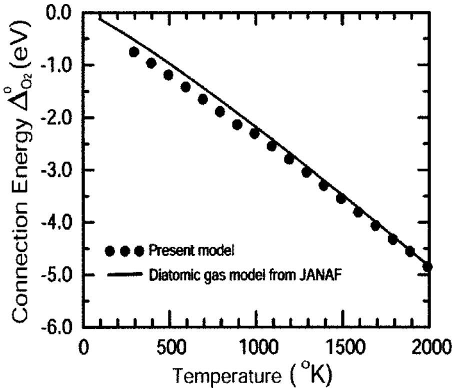

FIG. 1. Comparison of the oxygen-ambient connection energy $\Delta^0_{O_2}(T,p^0_{O_2}=1\text{ atm})$ from the present model [Eq. (14)] with that from the direct gas approach (JANAF tables, Refs. 8 and 35).

$$\Delta^0_{H_2O}(T,p^0_{H_2O}=1\text{ atm}) = \left(\frac{1}{z}\right)[\Delta H^{theo}_{A_xB_y}(0\text{ K}) - \Delta G^0_{A_xB_y\cdot zH_2O}(T) + \Delta^0_{A_xB_y\cdot zH_2O}(T) - \Delta^0_{A_xB_y}(T)]. \qquad (16)$$

Here $\Delta H^{theo}_{A_xB_y\cdot zH_2O}$ and $\Delta G^0_{A_xB_y\cdot zH_2O}$ correspond to the following reaction:

$$A_xB_y(\text{solid}) + zH_2O(\text{gas}) = A_xB_y\cdot zH_2O(\text{solid}). \qquad (17)$$

## III. DISCUSSION OF THE GASEOUS CONNECTION ENERGY

### A. Comparison with a more direct approach

A more direct but approximate approach[8] to determining the gas connection energy $\Delta^0_B(T,p^0_B=1\text{ atm})$ would be to carry out fundamental computations of the Gibbs energy of a molecular gas as a function of pressure and temperature. In fact this has already been done for a number of gases, and the results can be found in the JANAF tables.[35] Results of this procedure for $O_2$ are shown in Fig. 1. For comparison, results for the connection energy obtained from Eq. (14) are also plotted in Fig. 1. For this, solids $Al_2O_3$ and fcc Al are used as reference states, and data for $\Delta G^0_{Al_2O_3}(T)$ and the relevant specific heats are taken from Refs. 13 and 14. The *ab initio* heat of formation of $Al_2O_3$ was computed, and the value of 17.37 eV we obtained is consistent with earlier results.[7,9] One can see from Fig. 1 that results for the gas connection energy obtained via these quite different approaches are in good agreement. This is both satisfying and illuminating, revealing the connections between properties of gases and solids in thermodynamic equilibrium.

### B. Approximate expression for empirical gaseous connection energies

One can rewrite Eq. (14) as

$$\Delta^0_B(T_r,p^0_B=1\text{ atm}) = \left(\frac{1}{y}\right)T_r\Delta S^0_{A_xB_y}(T_r) + \left(\frac{1}{y}\right)[\Delta H^{theo}_{A_xB_y}(0\text{ K}) - \Delta H^0_{A_xB_y}(T_r) + \Delta^0_{A_xB_y}(T_r) - x\Delta^0_A(T_r)]. \qquad (18)$$

Note the evaluation is done at room temperature $T_r$ for purposes of this discussion. Because of the relatively small values of the terms $\Delta^o_i(T_r)$, and the relatively weak dependence of $\Delta H^0_{A_xB_y}$ on temperature for solids,[13] the terms in square brackets on the right-hand side of Eq. (18) can be neglected relative to the first term. This is exemplified for solid Al and $Al_2O_3$, where $\Delta^o_i(T_r)$ is −0.040 eV/atom for Al and −0.055 eV/formula unit for $Al_2O_3$.[14,35] The change of heat of formation from 0 K to room temperature is estimated to be 0.05 eV for Al and 0.1 eV for $Al_2O_3$.[35] Within this approximation the gaseous connection energy becomes

$$\Delta^0_B(T_r,p^0_B=1\text{ atm}) \cong \left(\frac{1}{y}\right)T_r\Delta S^0_{A_xB_y}(T_r). \qquad (19)$$

This is a particularly interesting relationship, because the gaseous connection energy is a property of the pure gas *B*, while it is taken to be approximately equal to the entropy of formation of the solid $A_xB_y$ from the solid *A* and gas *B*.

One can test the accuracy of Eq. (19) via thermodynamic data[14] for the entropy of formation of a variety of solids, shown in Table I. The data for solids formed from a given gas are grouped together. We did this because, if Eq. (19) were accurate, one would expect that data for the entropy of the formation of a variety of solids formed from a given gas would be approximately the same. One can see from Table I that this is approximately true. By Fig. 1 and Sec. III A, one might also wish to test Eq. (19) by a comparison of empirical entropies of formation with results of the direct computation of gaseous Gibbs energies as given by the JANAF tables. This is a direct comparison of the results of computations on a pure gas with empirical entropies of formation of solids. These computational results are listed in Table I as "JANAF," and one can see that they agree well with the entropies of formation. This is a particularly clear example of the interrelationship of gaseous and solid state properties under conditions of thermodynamic equilibrium.

## IV. STRUCTURE OF ULTRATHIN $Al_xO_y$ FILMS ON Al-DOPED Cu(111)

Next, the formalism developed here to connect *ab initio* results with thermodynamics is applied to the problem of examining possible structures of ultrathin aluminum oxide films on Al-doped Cu(111). The structure of such ultrathin $Al_xO_y$ films on metal surfaces has been the subject of considerable research over the last few years.[9,24,25,28–30] Experimentally, it was found that the $Al_xO_y$ structure is not the same as that of $\alpha$-$Al_2O_3$ when the film thickness is about 5 Å or less on a Ni-Al alloy surface,[28,29,37] and aluminum atoms could occupy octahedral as well as tetrahedral interstitial sites within the oxygen sublattice. For 5–7 Å $Al_xO_y$ films on Al(111), Mo(110), and Ru(001), Jennison,[36] Ver-

TABLE I. Empirical values of $(1/y)T_r\Delta S^0_{A_xB_y}(T_r)$ (eV/formula) for the formation of the solid $A_xB_y$ from the solid $A$ and gas $B$ as described by Eq. (11). $\Delta S^0_{A_xB_y}(T_r)$ is the room temperature entropy change associated with the formation of the solid. Nine representative gases are chosen and listed at the top of each column of data. The corresponding solid formed is listed to the left of each data value. The results are computed from thermodynamic data (Ref. 14). The average is the mean value of $(1/y)T_r\Delta S^0_{A_xB_y}(T_r)$ for the solids listed in the table. The results designated as JANAF are the values of connection energies based on the direct gas approach (Sec. III A) to the fundamental computation of the Gibbs energies of gases. The results for this are taken from the JANAF tables (Ref. 35).

| Solid | $\frac{1}{2}O_2$ | Solid | $\frac{1}{2}H_2$ | Solid | $H_2O$ |
|---|---|---|---|---|---|
| $Al_2O_3$ | −0.32 | $AlH_3$ | −0.20 | AlOOH(diasp) | −0.52 |
| $As_2O_3$ | −0.26 | $BaH_2$ | −0.20 | AlOOH(boch) | −0.44 |
| $Au_2O_3$ | −0.28 | $BeH_2$ | −0.19 | $Al_2O_3.3H_2O$ | −0.49 |
| BaO | −0.29 | $CaH_2$ | −0.20 | $Be(OH)_2$ | −0.47 |
| $Fe_2O_3$ | −0.28 | $MgH_2$ | −0.21 | $Cu(OH)_2$ | −0.45 |
| $RuO_2$ | −0.27 | $NdH_2$ | −0.22 | $NaSO_4.7H_2O$ | −0.47 |
| $SiO_2$ | −0.28 | $SrH_2$ | −0.21 | $NaSO_4.10H_2O$ | −0.45 |
| | | | | $ZnSO_4.H_2O$ | −0.47 |
| | | | | $ZnSO_4.2H_2O$ | −0.46 |
| Average | −0.28 | | −0.20 | | −0.47 |
| JANAF | −0.27 | | −0.16 | | −0.47 |
| Solid | $CO_2$ | Solid | CO | Solid | $1/2S_2$ |
| $Ag_2CO_3$ | −0.52 | $Mo(CO)_6$ | −0.46 | AsS | −0.27 |
| $BaCO_3$ | −0.55 | $Na_2CO_3$ | −0.49 | $As_2S_3$ | −0.26 |
| $MgCO_3$ | −0.54 | $SrCO_3$ | −0.49 | $B_2S_3$ | −0.27 |
| $MnCO_3$ | −0.51 | $W(CO)_6$ | −0.46 | BeS | −0.28 |
| $Na_2CO_3$ | −0.48 | | | $Bi_2S_3$ | −0.26 |
| $NiCO_3$ | −0.51 | | | CoS | −0.29 |
| | | | | CuS | −0.25 |
| | | | | FeS | −0.25 |
| Average | −0.52 | | −0.48 | | −0.27 |
| JANAF | −0.56 | | −0.52 | | −0.31 |
| Solid | $\frac{1}{2}N_2$ | Solid | $NO_2$ | Solid | NO |
| AlN | −0.32 | $Ba(NO_3)_2$ | −0.55 | $CsNO_3$ | −0.62 |
| BN | −0.27 | $KNO_3$ | −0.51 | $KNO_3$ | −0.62 |
| $Be_3N_2$ | −0.29 | $NaNO_3$ | −0.53 | $NaNO_3$ | −0.65 |
| $Ca_3N_2$ | −0.31 | | | | |
| GaN | −0.33 | | | | |
| InN | −0.34 | | | | |
| $Si_3N_4$ | −0.27 | | | | |
| Average | −0.30 | | −0.53 | | −0.63 |
| JANAF | −0.25 | | −0.64 | | −0.56 |

dozzi, Schultz, and Sears predicted a "$\tau$"-$Al_2O_3$ structure with two Al atoms occupying tetrahedral interstitial sites between two O layers within an fcc(111) $(\sqrt{3}\times\sqrt{3})$ unit cell.

Well-ordered $Al_2O_3$ films were grown on Al-doped Cu(111) surfaces recently.[30] The thickness of the $Al_2O_3$ films was estimated[30] to be 35 Å. In view of the aforementioned different ultrathin film $Al_xO_y$ structures observed on NiAl(110) surfaces, it would be interesting to employ the methods to connect thermodynamics and *ab initio* computations to help sort through such potential structures on Al-doped Cu(111) surfaces. This may precipitate experimental investigations of ultrathin ($\lesssim$10 Å) $Al_xO_y$ films on Al-doped Cu(111) surfaces. Ultrathin $Al_xO_y$ layers on Cu(111) surfaces of two different $Al_xO_y$ thin film thicknesses were considered, one containing two oxygen layers and the other containing three, both films adhered to Cu(111) surfaces. Both hcp and hex stackings of the oxygen layers were studied for the three oxygen-layer-thick films. Different numbers of Al

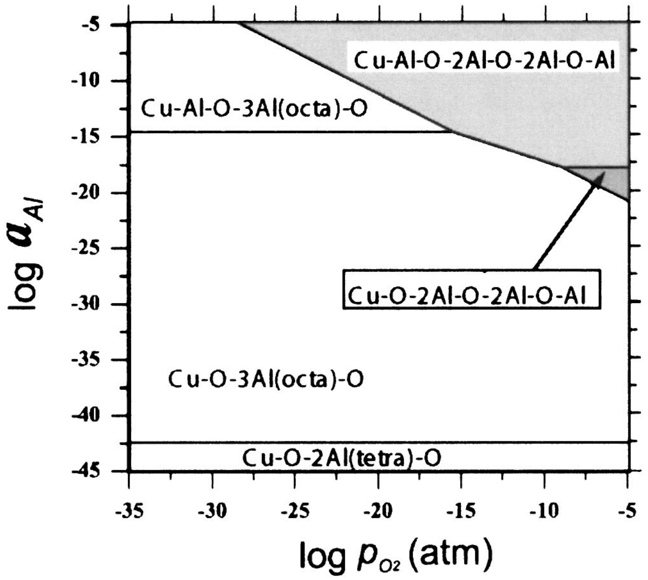

FIG. 2. Phase diagram (as a function of the Al activity and ambient oxygen partial pressure) for ultrathin $Al_xO_y(0001)$ films on Al-doped Cu(111). A temperature of 1200 K is assumed and logarithms are to the base 10.

atoms were inserted at the octahedral and/or tetrahedral interstitial sites within the oxygen sublattice to simulate the many possible structures. The O layer closest to the Cu(111) surface is placed at an fcc site of a Cu(111) surface. All computations are performed via VASP, a plane wave electronic structure computational package,[38] employing ultrasoft pseudopotentials.[39] For a discussion of approximations made in this computation, see Ref. 10.

For the films with two oxygen layers and a $(\sqrt{3}\times\sqrt{3})$ fcc unit cell, which is the same unit cell as that of Cu(111), inserting two Al atoms (per unit cell) at tetrahedral interstitial sites leads to the so-called "$\tau$"-$Al_2O_3$ structure [labeled by atomic layer here and in Fig. 2 as Cu-O-2A1(tetra)-O], and placing three Al atoms (per cell) at octahedral interstitial sites gives the structure labeled here and in Fig. 2 as Cu-O-3A1(octa)-O. Note that for both of these two oxygen layer cases, the $Al_xO_y$ thin films are all O-terminated at their free surfaces. Again, these choices were motivated by structures observed[28,29,37] for ultathin $Al_xO_y$ films grown on Ni-Al alloy surfaces.

By the structure labeled as Cu-Al-O-2Al-O-2Al-O-Al in Fig. 2, we mean that the three oxygen layers are in a hcp structure, and all Al atoms are at octahedral interstitial sites as in the $\alpha$-$Al_2O_3$ structure.[40,41] In addition, in this case both the film surface and the Cu/$Al_xO_y$-film interface are Al terminated. By the designation Cu-O-2A1-O-2A1-O-Al in Fig. 2, we mean that the structure is similar to the Cu-Al-O-2A1-O-2A1-O-Al but with an O-terminated Cu/$Al_xO_y$-film interface.

For all of these Cu(111)/$Al_xO_y$ interfaces, commensuration is assumed, but two different interfacial lattice constants (with different interfacial strain) are considered. The first interfacial lattice constant is that of bulk Cu(111), and another one is that of bulk $\alpha$-$Al_2O_3(0001)$. It turns out that the interfacial phase diagram (Fig. 2) is not sensitive to these two different interfacial strains. The results presented there are for the lattice constant of bulk $\alpha$-$Al_2O_3$. A temperature of 1200 K is assumed. Readers may refer to our earlier publications[10] for details of our computational methods.

Because there is no bulk $Al_2O_3$ reservoir to come to equilibrium with in this case, unlike the cases considered in Sec. II B 1, the activity of aluminum and the partial pressure of oxygen are two independent variables controlling the film formation. From a practical standpoint, the oxygen partial pressure could be varied by controlling the ambient gas composition, while the aluminum activity is most easily varied by varying the doping of the bulk Cu with a few atomic percent of Al (see, e.g., Ref. 30). Consider the following equilibrium reaction:

$$\mathrm{Cu/Al}_x\mathrm{O}_y + m\mathrm{Al} + \left(\frac{n}{2}\right)\mathrm{O}_2 \leftrightarrows \mathrm{Cu/Al}_{x+m}\mathrm{O}_{y+n}. \tag{20}$$

The Gibb's energy is conserved because of the assumed thermodynamic equilibrium [see also Eqs. (4) and (5)]:

$$m\,kT\ln a_{Al} + \left(\frac{n}{2}\right)kT\ln p_{O_2} = \Delta G_{\mathrm{Re}}, \tag{21}$$

with

$$\begin{aligned}\Delta G_{\mathrm{Re}} = {} & \left[G_{Cu/Al_{x+m}O_{y+n}} - G_{Cu/Al_xO_y} - m\mu_{Al}^{0}(0\ \mathrm{K})\right] \\ & - \left(\frac{n}{2}\right)\mu_{O_2}^{0}(0\ \mathrm{K},\mathrm{isolated}) - m\Delta_{Al}^{0}(T) \\ & - \left(\frac{n}{2}\right)\Delta_{O_2}^{0}(T,1\ \mathrm{atm}).\end{aligned} \tag{22}$$

The resulting phase diagram for the $Al_xO_y$ thin film on a Cu(111) surface as shown in Fig. 2. Results are plotted there for a representative temperature $T=1200$ K and for oxygen partial pressures up to $10^{-5}$ atm. For this temperature, at higher oxygen partial pressures on would expect [42] the formation of $CuAlO_2$, and CuO at still higher oxygen partial pressures. Considering first the two-oxygen-layer $Al_xO_y$ thin films, it is noticed that the so-called "$\tau$"-$Al_2O_3$ structure [labeled in Fig. 2 as Cu-O-2Al(tetra)-O], is the dominant phase when the Al activity is relatively low. In particular, as the Al impurity percentage in the bulk Cu decreases, the Al activity also decreases. As the Al impurity percentage approaches zero (to pure Cu), the Cu-O-2A1(tetra)-O phase becomes the only phase. As the Al impurity percentage in the Cu increases from zero, one can see from Fig. 2 that at a very low Al activity $a_{\mathrm{Al}}$ (and a correspondingly very low Al doping), the structure of the thin film with two oxygen layers changes from the Cu-O-2A1(tetra)-O phase to the Cu-O-3Al(octa)-O phase, i.e., having a monolayer of Al atoms occupy all octahedral sites between the two oxygen layers. In the case of a relatively low oxygen pressure and a substantially higher Al activity, the Cu-Al-O-3Al(octa)-O structure is also possible, again as shown in Fig. 2. Many other configurations with different combinations of Al occupancies of the two oxygen layers were investigated, but none were found to have lower energies than any of the three structures discussed here and included in Fig. 2.

With the thickness of the film increased to three oxygen layers, the stable structures become $\alpha$-$Al_2O_3$-like. Cu/$Al_xO_y$ films that have next to the outermost Cu atomic layer either an Al atomic layer (Cu-Al-O-2A1-O-2Al-O-Al) or an O atomic layer (Cu-O-2A1-O-2A1-O-Al) may be obtained, and the free surfaces of all these $Al_xO_y$ films stabilize at Al termination. One can compare the $Al_xO_y$ film structure with that of the pure $Al_2O_3(0001)$ surface at equilibrium with an $Al_2O_3$ bulk. The inward relaxation of the outermost Al layer of the $Al_xO_y$ film (−92% relative to the bulk spacing between the outermost Al layer and the O layer next to it), is a little larger than that[40] of the pure $Al_2O_3(0001)$ surface (−86%), and the separation between the two Al layers below the outermost O layer becomes essentially zero within our numerical accuracy instead of the 0.29 *Å* spacing obtained[7,9,40] for the pure $Al_2O_3(0001)$ surface. The portions of the phase diagram allocated to the two structures are shown in Fig. 2. As expected, the Cu-Al-O-2A1-O-2A1-O-Al structure occurs at higher Al activities $a_{Al}$ and lower oxygen partial pressures $p_{O_2}$ than the Cu-O-2A1-O-2A1-O-Al structure. These structures are similar to what we found[10,41] for thick $Al_2O_3$ and Cu slabs. The former structure is similar to what we called the Al-terminated interface and as denoted by $Cu/(Al_2O_3)_{Al}$ for the thick slabs, while the latter is similar to the O-terminated interface denoted as $Cu/(Al_2O_3)_O$. These results imply that the $Al_xO_y$ film should contain at least three O layers if one wishes to simulate thick $\alpha$-$Al_2O_3$/metal interfaces.

This analysis of ultrathin $Al_xO_y$ films on Cu-Al alloy surfaces is not meant to be exhaustive, as there are many more possible structures than were examined here. Rather, it is meant to be illustrative of how one might connect metallurgical or thermodynamic analyses with *ab initio* computations.

## V. SUMMARY

In this manuscript a bridge has been established between the variables and standard states of *ab initio* computations and the variables and standard states of thermodynamics. This is a potentially powerful link, expanding the predictability of the *ab initio* methods and the fundamental understanding of thermodynamics. The *ab initio* and thermodynamic or metallurgical standard states are linked by connection energies. Connection energies for solids are obtained via temperature integrations over empirical specific heats and entropies. Connection energies for gases can be obtained either from properties of the solids, which are in thermodynamic equilibrium with the gases or directly from gaseous properties, and there is good agreement between the two approaches. This led to the discovery that the formation entropy of compounds formed at a given temperature from a given gas and a variety of solids should be approximately constant. Relations are derived between the *ab initio* variables, which are the chemical potentials, and the thermodynamic or metallurgical variables, which are the activities and partial pressures. Finally, a phase diagram is computed for ultrathin $Al_xO_y$ films on Al-doped Cu(111), two or three oxygen layers thick and with a variety of Al atom layer locations.

## ACKNOWLEDGMENTS

The authors are grateful for partial ONR support under Grant No. N00014-99-l-0170 and for useful comments from Professor Anthony Evans.

---

[1] G. X. Qian, R. M. Martin, and D. J. Chadi, Phys. Rev. B **38**, 7649 (1988).
[2] I. N. Remediakis, E. Kaxiras, and P. C. Kelires, Phys. Rev. Lett. **86**, 4556 (2001).
[3] S. B. Zhang, and J. E. Northrup, Phys. Rev. Lett. **67**, 2339 (1991).
[4] Y. Yang, S. B. Zhang, and S. T. Pantelides, Phys. Rev. Lett. **86**, 5723 (2001).
[5] J. Padilla and D. Vanderbilt, Phys. Rev. B **56**, 1625 (1997).
[6] X.-G. Wang, W. Weiss, Sh. K. Shaikhutdinov, R. Ritter, M. Petersen, F. Wagner, R. Schlogl, and M. Scheffler, Phys. Rev. Lett. **81**, 1038 (1998).
[7] X.-G. Wang, A. Chaka, M. Scheffler, Phys. Rev. Lett. **84**, 3650 (2000).
[8] K. Reuter and M. Scheffler, Phys. Rev. B **65**, 035406 (2001).
[9] W. Zhang, and J. R. Smith, Phys. Rev. B **61**, 16883 (2000); Phys. Rev. Lett. **85**, 3225 (2000).
[10] W. Zhang, J. R. Smith, and A. G. Evans, Acta Mater. **50**, 3803 (2002).
[11] I. G. Batirev, A. Alavi, and M. W. Finnis, Phys. Rev. B **62**, 4698 (2000).
[12] P. Mahadevan and A. Zunger, Phys. Rev. Lett. **88**, 047205 (2002).
[13] D. R. Gaskell, *Introduction to Metallurgical Thermodynamics*, 2nd ed. (McGraw-Hill, New York, 1981); D. R. Gaskell, in *Physical Metallurgy*, edited by R. W. Cahn and P. Hassen (Elsevier Science, Amsterdam, 1996), Chap. 5.
[14] O. Kubaschewski, C. B. Alcock, and P. J. Spencer, *Materials Thermochemistry*, 6th ed. (Pergamon, Oxford, 1993).
[15] G. Burns, *Solid State Physics* (Academic, New York, 1985); J. W. Whalen, *Molecular Thermodynamics: A Statistical Approach* (Wiley, New York, 1991).
[16] A. G. Evans, D. R. Mumm, J. W. Hutchinson, G. H. Meier, and F. S. Pettit, Prog. Mater. Sci. **46**, 505 (2001).
[17] E. Saiz, R. M. Cannon, and A. P. Tomsia, Acta Mater. **47**, 4209 (1999).
[18] D. Chatain, L. Coudurier, and N. Eustathopoulos, Rev. Phys. Appl. **23**, 1955 (1988).
[19] U. Alber, H. Mullejans, and M. Ruhle, Micron **30**, 101 (1999).
[20] V. Merlin and N. Eustathopoulos, J. Mater. Sci. **30**, 3619 (1995).
[21] K. P. Trumble and M. Ruhle, Acta Metall. Mater. **39**, 1915 (1991).

[22] K. P. Trumple, Acta Metall. Mater. **40**, S105 (1992).

[23] S. R. Morrison, *The Chemical Physics of Surfaces*, 2nd ed. (Plenum, New York, 1990).

[24] P. J. Eng, T. P. Trainor, G. E. Brown, Jr., G. A. Waychunas, M. Newville, S. R. Sutton, and M. L. Rivers, Science **288**, 1029 (2000).

[25] G. E. Brown, Jr., V. B. Henrich, W. H. Casey, D. L. Clark, C. Eggleston, A. Felmy, D. W. Goodman, M. Gratzel, G. Maciel, M. I. McCarthy, K. H. Nealson, D. A. Sverjensky, M. F. Toney, and J. M. Zachara, Chem. Rev. (Washington, D.C.) **99**, 77 (1999).

[26] A. Munkholm, G. B. Stephenson, J. A. Eastman, C. Thompson, P. Fini, J. S. Speck, O. Auciello, P. H. Fuoss, and S. P. DenBaars, Phys. Rev. Lett. **83**, 741 (1999).

[27] J. Smialek and I. Glenn, in *Physical Metallurgy*, edited by R. W. Cahn and P. Hassen (Elsevier Science, Amsterdam, 1996), Chap. 14; A. G. Evans (private communication).

[28] M. Baumer and H. J. Freund, Prog. Surf. Sci. **61**, 127 (1999), and references cited therein.

[29] G. Geballos, Z. Song, J. I. Pascual, H.-P. Rust, H. Conrad, M. Baumer, and H.-J. Freund, Chem. Phys. Lett. **359**, 41 (2002).

[30] M. Yoshitake, S. Bera, and Y. Yamauchi, Surf. Interface Anal. **35**, 824 (2003); see also Y. Jeliazova and R. Franchy, Appl. Surf. Sci. **187**, 51 (2002).

[31] P. D. Tepesch and A. A. Quong, Phys. Status Solidi B **217**, 377 (2000).

[32] P. Liu, T. Kendelewicz, G. E. Brown, Jr., E. J. Nelson, and S. A. Chambers, Surf. Sci. **417**, 53 (1998).

[33] If the reference gas cannot be accurately approximated as an ideal gas, the relationship between partial pressure and activity of a constituent becomes more complicated. But the relationship between them can still be obtained without difficulty. See Ref. 13 for details.

[34] J. Pople, Rev. Mod. Phys. **71**, 1267 (1999); W. Kohn, *ibid.* **71**, 1253 (1999).

[35] M. W. Chase, C. A. Davies, J. R. Downey, D. J. Frurip, R. A. McDonald, and A. N. Syverud, JANAF Thermochemical Tables, 3rd ed. [J. Phys. Chem. Ref. Data **14**, 61 (1985)].

[36] D. R. Jennison, C. Verdozzi, P. A. Schultz, and M. P. Sears, Phys. Rev. B **59**, R15605 (1999).

[37] A. Stierle, F. Renner, R. Streitel, H. Dosch, W. Drube, and B. C. Cowie, Science **303**, 1652 (2004).

[38] G. Kresse and J. Hafner, Phys. Rev. B **47**, R558 (1993); G. Kresse and J. Furthmuller, Phys. Rev. B **54**, 11169 (1996).

[39] D. Vanderbilt, Phys. Rev. B **41**, 7892 (1990); G. Kresse and J. Hafner, J. Phys.: Condens. Matter **6**, 8245 (1994).

[40] See Table I of J. R. Smith and W. Zhang, Acta Mater. **48**, 4395 (2000).

[41] X.-G. Wang, J. R. Smith, and M. Scheffler, Phys. Rev. B **66**, 073411 (2002); J. Am. Ceram. Soc. **86**, 696 (2003); See also X. G. Wang, J. R. Smith, and A. Evans, Phys. Rev. Lett. **89**, 286102 (2002); W. Zhang, J. R. Smith, X. G. Wang, and A. G. Evans, Phys. Rev. B **67**, 245414 (2003).

[42] R. B. Gall and D. P. Cann, Ceram. Eng. Sci. Proc. **24**, No. 4, 1043 (2003).